Effect of pressure quenching on the structures and properties of borosilicate glasses: insights from molecular dynamics simulations

Mengguo Ren and Jincheng Du*

Department of Materials Science and Engineering, Department of Materials Science and Engineering, University of North Texas, Denton, Texas, USA

(*Corresponding author. Email: du@unt.edu)

Abstract:

Combining thermal and pressure effect represents a novel approach to modify glass properties. However, the microscopic structural origin is complex and far from fully understood, especially in glasses with mixed glass formers. We have utilized classical molecular dynamics simulations to investigate pressure-quenching effect on sodium borosilicate glasses. Hot compression, cold compression and annealing on the structures and properties are investigated and compared. It was found that applying pressure up to 10 GPa at the glass transition temperature led to permanent densifications and a dramatic increase of elastic moduli by 90%. The main structural change is the increase of four-fold coordinated boron while silicon remains four-fold coordinated. The sodium environment shows an increase of coordination number and a decrease of Na-O and Na-Na bond distances. Medium range structure is also changed with an increase of 8-membered rings. These results provide atomistic insights of the pressure quench effect on borosilicate glasses.

Key words: borosilicate glass, pressure effect, hot compression, mechanical properties, molecular dynamics, glass structure

1. Introduction

Applying pressure has become an novel method to control and manipulate glass properties in addition to commonly used thermal history and composition variations of glasses [1, 2]. Glass is a metastable solid formed from rapid quenching of liquid or melt. The structures and properties of

a glass are known to be sensitive to its thermal history such as cooling rate, annealing temperature and duration, which have been commonly used by glass scientists and engineers to optimize glass properties [3]. It has been recently discovered that pressure history can also affect the short and medium range glass structures, and consequently various glass properties [4,5]. For example, Svenson et al. found that applying pressure changed the ion diffusivity, which impacted the compressive stress and hardness in ion-exchanged aluminosilicate glasses [6]. It becomes clear that pressure history can be an additional control parameter, in addition to composition and thermal history, to manipulate and optimize glass properties [1, 2]. These changes are associated with the short and medium range structure changes of the glasses, as shown by in situ and ex situ characterization techniques. Nevertheless, the origin of these property changes due to coupled pressure and temperature fields is far from fully understood. For instance, thermal annealing and pressure both can induce densification but the underlying mechanism of densification can be very different [4]. In this work we apply classical molecular dynamics simulations to understand pressure quenching induced changes of properties in sodium borosilicate glasses and explore the origin of these changes in the pressure history induced short and medium range structural changes in these glasses. These results provide atomistic insights on the pressure quenching induced changes in network forming glasses with mixed glass formers.

Pressure induced changes in borate and borosilicate glasses have been extensively studied experimentally [1,2]. Two methods to apply pressure are commonly used: hot compression where temperature is applied up to the glass transition temperature during compression and the cold compression in which pression is applied at ambient temperature [2]. The range of pressure applied depends on the apparatus used to apply to pressure and can reach tens to 150 GPa for cold compression [2]. While due to limitation of the maximum temperature the pressure apparatus can withstand, hot compression usually happens at much lower pressure, e.g. 1-3 GPa. As pressure induced structural change in network glasses can happen at lower pressure at elevated temperatures [2], hot compression can achieve permanent changes of the glass and the method can be applied to larger sample sizes hence is of more practical importance. Pressure induced structural changes in boron oxide and borate glasses have been extensively investigated by using ¹¹B solid state NMR. In boron oxide glass, applied pressure led to gradual increase of boron coordination up 23 GPa, while for higher pressure in the 40 to 120 GPa range, only four-fold coordinated boron was observed [7]. Although higher pressure range (>3 GPa) is important for fundamental research,

available apparatus to achieve such higher pressure is limited to small sample sizes, with which fewer properties can be characterized. On the other hand, lower pressure (1-3 GPa) can be achieved for large samples and is of more technological importance and relevance. Wu et al. investigated pressure quenching effect on mechanical properties of a series of calcium aluminoborosilicate glasses [8,9]. Ex situ ¹¹B and ²⁷Al solid state NMR studies found that under the pressure of 1-3 GPa, both boron and aluminum coordination numbers increase with pressure for samples under hot compression and for glasses with higher boron oxide amount showed higher recoverable densification, while samples under cold compression led to no changes of aluminum coordination [9]. Hot compression has also led to increase of Young's moduli and hardness and these property changes were correlated the atomic packing density [9].

Molecular dynamics and related atomistic simulations have been developed in to highly valuable methods to elucidate the structures and structure-property relations of inorganic glass materials [10]. Despite its wide application in studying silicate glass structures, MD simulations of borate and borosilicate glasses are rather limited [11,12], mainly due to the availability of reliable empirical potentials for borate containing glasses where there exists a more complex structure change with composition as compared to silicate glasses. Recent developments of effective potentials have enabled the simulations of borosilicate and other boron containing multicomponent glasses [13–16]. There are several potentials developed borosilicate glass systems, the one developed by Kieu et al. [17] and further expanded by Deng and Du [18] has composition dependent partial atomic charges to account for the different ratio of three- and four-fold coordinated boron. The short range interaction has the Buckingham form with the B-O parameters also vary with composition. The resulting potential gives accurate boron coordination change with composition that is consistent with the Dell-Bray-Xiao model [19] and provides mechanical properties that are in good agreement with experimental values. This set of pairwise partial charge potential also has the advantage of computational efficiency. Due to these reasons, this set of potential was adopted in this work to understand pressure effect on structure and properties of a sodium borosilicate glass. Kilymis et al. have used the same potential to study the densification of sodium borosilicate glasses after compression/decompression for isostatic pressure up to 20 GPa [20]. The result shows a linear increase of bulk modulus for pressure up to 15 GPa. It was found that atomic packing is the main reason behind the amount of densification. Pronounced shortening of Na-Na and Na-O bond distances were also observed during compression. Recently, hot and cold

compression effect on two commercial borosilicate glasses were investigated by MD simulations using two interatomic potentials [21,22]: the Deng and Du potential [23] and Wang et al. [15] potential. It was found that boron coordination change and bond angle variations are the dominating factors of pressure induced structural changes.

The paper is arranged in the following way: in the next section, simulation methodologies including empirical potential employed and glass forming and pressure quench procedures are described. This is followed by the results section where the structure and property changes due to pressure quenching and annealing are reported. These results are compared with those of the as formed glass and from room temperature pressing. This is followed by the discussion and conclusion sections.

2. Simulation methodologies

Sodium borosilicate glass structures were generated using a simulated melt and quench process with MD simulations. Three independent glass samples with different initial random configurations were generated for each composition to obtain statistics of the simulated properties and structures information. The initial random configurations were firstly energy minimized at 0K to remove unreasonable structures, e.g., atom pairs that were too close to each other. After further relaxation at 300 K for 60ps, the systems temperature were increased to 6000 K for 60 pico-second (ps) to fully melt the glass. The melt was then equilibrated 5000 K for 100 ps to before quenching to 300 K with a cooling rate of 0. 2 K/ps. Canonical ensemble (NVT) was used during the melt and quench process with a 1 femto-second (fs) time step. The generated glass structures were then relaxed at 300 K using constant pressure (NPT ensemble) simulations at ambient pressure to relieve the stress. The relaxed glass structures were further equilibrated at 300 K under microcanonical (NVE) ensemble for 100 ps, with configurations recorded in the last 60 ps every 50 fs for final structural analysis. All the simulations were carried by using the DL_POLY simulation package [24]. Long range Coulombic forces were calculated using the Ewald summation method with a precision of 10⁻⁶ eV.

Recent active developments have led to several interatomic potentials that can be used for the simulations of borosilicate and other boron oxide containing glasses. Two general types of potentials were developed: fixed charge and parameter potential and composition dependent potential. The interatomic potentials we chose to use in this work were based on a set of partial charge pairwise potentials for silicate minerals and magma developed by Guillot and Sator [25]. These potentials were expanded by Kieu et al. [26] to borosilicate glasses and by Deng and Du [18] to boroaluminosilicate glasses by introducing composition dependent atomic charges and B-O short range parameters that enable description of boron coordination change with glass composition. This potential consists the long range Coulombic interactions, where partial atomic charges were used, and the short range interactions with the Buckingham form:

$$\Phi(r_{ij}) = \frac{q_i q_j}{r_{ij}} + A_{ij} e^{\frac{-r_{ij}}{\rho_{ij}}} - \frac{c_{ij}}{r_{ij}^6}$$
 (1)

where, r_{ij} is the distance between atom pair i and j; the q_i and q_j values are the calculated effective charges for atom pair i and j based on the composition, respectively. A_{ij} , ρ_{ij} and C_{ij} are the empirical parameters for the Buckingham term. One important feature of this potential set is the composition-dependent atomic charges, where three and four-fold coordinated boron has different charges based on first principles calculations and the average charge of boron is obtained based on the four-fold coordination of boron predicted from the Yun, Dell and Bray (YDB) model [19]. The charges of other atoms were then scaled accordingly. Additionally, the Buckingham A parameter of the B-O pair in the Buckingham term is also composition-dependent. Details of the potential form and list of the parameters can be found in Ref. [18]. Although later investigations found some limitation of the potential, especially for large R values due to the potential form¹⁶, the composition range investigated in this work can be well reproduced by the potential. An additional reason to choose the potential is due to the fact that the potential was able to accurately reproduce mechanical properties of a series of borosilicate glasses [16, 24]. Furthermore, the potential has been successfully used to study pressure effect on a series of sodium borosilicate glasses up to 20 GPa [20].

A series of simulation experiments on pressure quenching, cold compression and subsequent annealing were performed in the selected borosilicate glasses using MD simulations. Constant pressure (NPT) ensemble with the Berendson thermal and barostat was used in all the simulations involving pressure effect. The procedure of simulated pressure quenching involved four steps: (a) the glass formed from the simulated melt and quench process was first heated to around T_g+150 K (T_g determination described in section 3.1) at 10 GPa applied pressure with a heating rate of 2 K/ps (pico-second), (b) the compressed glass was equilibrated at T_g at 10 G Pa for 2 nano-seconds (2x10⁶ steps), (c) the pressured glass was cooled down to 300 K to 300 K under 10 GPa pressure

with a cooling rate of 2 K/ps, (d) the pressure quenched glass was relaxed at 300 K and 1 atmospheric pressure for 120 ps. The procedure for the pressure quenching process is shown in Fig. 1.

Furthermore, the effect of thermal annealing of pressured samples and room temperature pressure (cold pressing) on the sodium borosilicate glasses were also studied. To understand the effect of thermal annealing on the glass structure, the pressure quenched glass went through a relaxation at Tg and ambient pressure for 2 nano-seconds and was then cooled down to 300 K with 2 K/ps to generate the annealed glass sample. For comparison of the above glasses under hot compression, a glass under cold compression was studied that it was compressed at room temperature to 10 GPa and the pressure was decreased to ambient pressure with the same length of simulation as in the above mentioned procedures. The glass structures were monitored in the pressure and depressurize processes. The final glass structures of the as formed, pressure quenched, annealed, and room temperature pressure quenched glass were analyzed. These glasses were named original, pressure-quenched, room temperature pressure (RT), and annealed, respectively. For each condition, three independent glass samples were prepared to obtain statistics of the structures and properties.

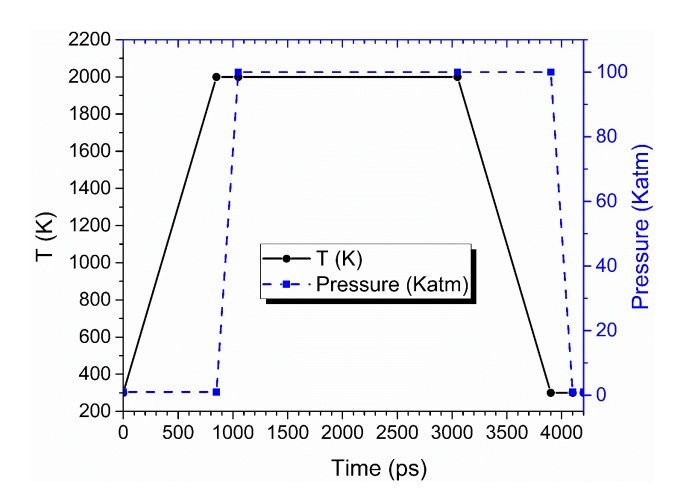


Fig. 1 Temperature and pressure profile as a function of simulation time for pressure quenched glass.

3. Results

3.1 Structures of sodium borosilicate glasses from MD simulations

To evaluate the effectiveness of the potentials, a series of sodium borosilicate glasses (Table 1) with the same K (SiO₂/B₂O₃) value (K=2) but different R (Na₂O/B₂O₃) values ranging from 0.1 to 0.5 have been simulated using the MD simulations with the potential and procedure detailed in the previous section. The total atom number in each cubic simulation cell was around 6,000 (Table 1). In this study, we use a cooling rate of 0.2 K/ps, while glasses formed with a higher cooling rates (5 K/ps) of same glass compositions were used for comparison [18]. To figure out the cooling rate effect, the four-fold coordinated boron fraction (N₄) was calculated and compared with the theory data calculated by Yun, Dell and Bray (YDB) model [19]. As shown in Fig. 2, the difference of N₄ between glasses generated with two cooling rates is fairly small, with both match well with the YDB model. These results indicated that this potential works well for these glass compositions (lower R value) and was able to obtain reasonable glass structure within a relatively large range of cooling rate. Our recent study showed that in MD simulations of borosilicate glasses, the boron N₄ value depends on the system size and cooling rate. While a system size with over 1600 atoms were shown to be able to converge the N₄ and other structure parameters. Hence the system size of 6000 atoms used in this work was sufficient to observe the structural changes due to pressure quenching effect.

Table 1 Composition, density and simulation cell details of the sodium borosilicate glasses studied

SiO ₂	Na ₂ O	B_2O_3	Exp. <i>ρ</i> [27]	R	K	Atom # used in MD			
	(mol%)		(g/cm^3)	(Na_2O/B_2O_3)	(SiO_2/B_2O_3)	O	В	Na	Si
64.5	3.2	32.2	2.098	0.1	2	3776	1068	96	1063
62.5	6.3	31.3	2.147	0.2	2	3727	1038	208	1033
60.6	9.1	30.3	2.237	0.3	2	3679	1008	302	1008
58.8	11.8	29.4	2.308	0.4	2	3641	984	394	984
57.1	14.3	28.6	2.396	0.5	2	3598	962	482	957
	64.5 62.5 60.6 58.8	(mol%) 64.5 3.2 62.5 6.3 60.6 9.1 58.8 11.8	(mol%) 64.5 3.2 32.2 62.5 6.3 31.3 60.6 9.1 30.3 58.8 11.8 29.4	[27] (mol%) [27] (g/cm³) 64.5 3.2 32.2 2.098 62.5 6.3 31.3 2.147 60.6 9.1 30.3 2.237 58.8 11.8 29.4 2.308	[27] (mol%) [27] (g/cm³) (Na ₂ O/B ₂ O ₃) 64.5 3.2 32.2 2.098 0.1 62.5 6.3 31.3 2.147 0.2 60.6 9.1 30.3 2.237 0.3 58.8 11.8 29.4 2.308 0.4	[27] (mol%) [27] (g/cm³) (Na ₂ O/B ₂ O ₃) (SiO ₂ /B ₂ O ₃) 64.5 3.2 32.2 2.098 0.1 2 62.5 6.3 31.3 2.147 0.2 2 60.6 9.1 30.3 2.237 0.3 2 58.8 11.8 29.4 2.308 0.4 2		[27] (mol%) [27] (g/cm³) (Na ₂ O/B ₂ O ₃) (SiO ₂ /B ₂ O ₃) O B 64.5 3.2 32.2 2.098 0.1 2 3776 1068 62.5 6.3 31.3 2.147 0.2 2 3727 1038 60.6 9.1 30.3 2.237 0.3 2 3679 1008 58.8 11.8 29.4 2.308 0.4 2 3641 984	[27] (mol%) [27] (g/cm³) (Na ₂ O/B ₂ O ₃) (SiO ₂ /B ₂ O ₃) O B Na 64.5 3.2 32.2 2.098 0.1 2 3776 1068 96 62.5 6.3 31.3 2.147 0.2 2 3727 1038 208 60.6 9.1 30.3 2.237 0.3 2 3679 1008 302 58.8 11.8 29.4 2.308 0.4 2 3641 984 394

Fig. 3(a) shows the system configurational energy versus temperature during the heating process using constant volume simulations with a 0.2 K/ps cooling rate. Based on the point at which there is a slope change (Fig. 3(a)), the glass transition temperature for each sample were estimated and summarized in Fig. 3(b). Although the T_g from simulation are higher than

experimental values, which were a result of the artifact of adopted potentials. The results show that T_g decreases with the increase of the R value, consistent with experimental observations [28].

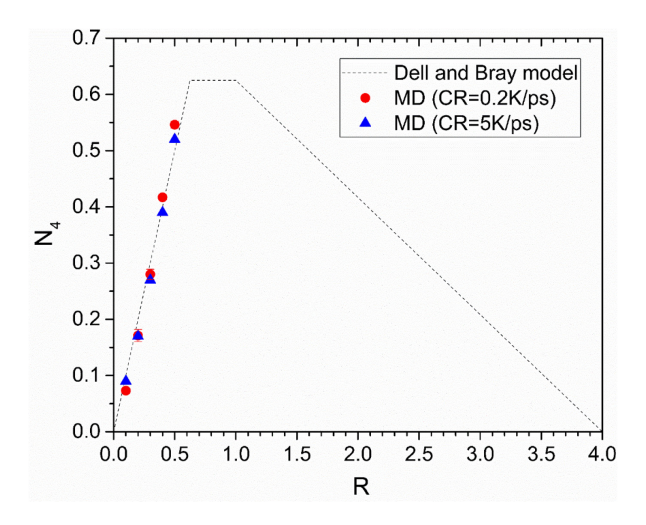


Fig. 2 Four-fold coordinated boron fraction (N₄) as a function of R (Na₂O/B₂O₃) for MD simulated glass with two cooling rates (5 K/ps¹⁶ and 0.2 K/ps) and those from the Yun, Dell and Bray model (dash line).

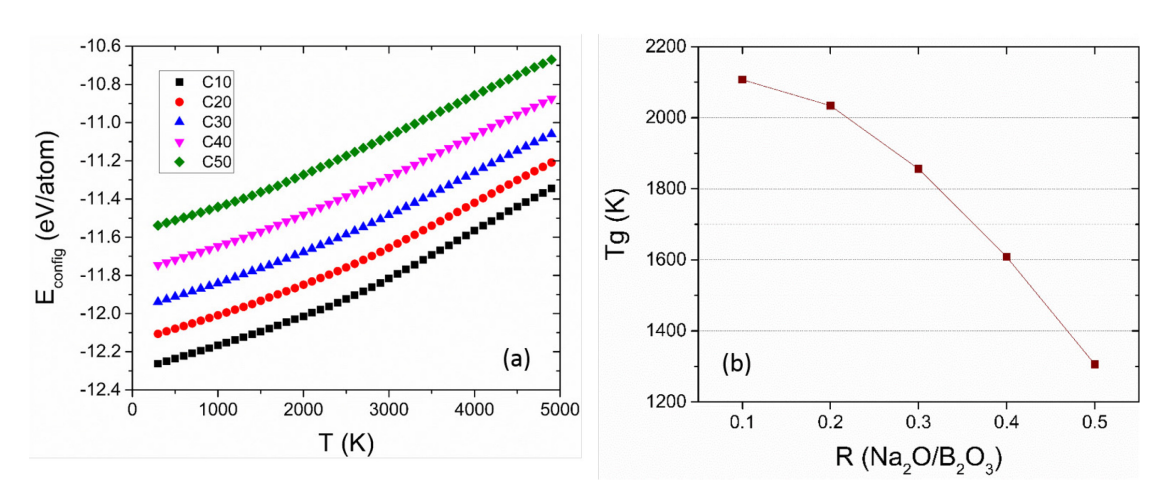


Fig. 3 (a) Configuration energy versus temperature and (b) $T_{\rm g}$ as a function of composition (R) in simulated borosilicate glasses

To study the effect of pressure quenching on the structure and properties of borosilicate glass, we choose the C30 sample (see Table 1 for glass composition) as a representative. Considering the $T_{\rm g}$ for C30 sample is around 1850 K, the temperature used for pressure quench process was chosen to be 2000 K to ensure an obvious irreversible structure change after decompression. The procedure for pressure quenching process has elaborated in the methodologies section.

3.2 Effect of pressure and thermal history on glass structures

Glasses under compression usually undergo densification. The underlying structural changes can be complex. In borosilicate glasses, boron coordination change has been observed in glasses under compression. Fig. 4 shows the boron N₄ and glass density change during the pressure quenching process. It can be seen that in the compression and heating process, the density change and boron N₄ values are closely correlated. As expected, glass density (plotted in terms of ρ/ρ_0) gradually decreases during the initial heating (Fig. 4a) from room temperature to around T_g and then during the depressurizing process (Fig. 4d). On the contrary, applying pressure at around T_g (Fig. 4b) and cooling under pressure (Fig. 4c) leads to an increase of glass density. During the whole pressure quenching process, N₄ changes are in similar trend with glass density. The glass density ratio (ρ/ρ_0) increased from 1 to 1.18 while N₄ increased from 28% to 38%. These results confirm that in borosilicate glasses, increase of boron coordination is one of the main mechanisms of densification [8, 9]. These results also show that the adopted interatomic potentials are capable to describe the structural changes of borosilicate glasses under pressure. Further studies of short and medium range structure changes due to hot compression in comparison with those under cold compression and changes of glass properties will be reported in next sections.

Table 2 Summary of short range glass structures of samples before and after pressure quenching and annealing. (Original: glass as formed from MD simulations; pressure quenched: glass undergone through 10 GPa pressure at 2000 K; pressure-RT: glass was pressured to 10GPa at room temperature; Annealed: pressure quenched glass was further annealed at around Tg and the cooled to room temperature.)

	O species (%)		Si-Q _n species (%)			B-Q _n species (%)			B N ₄	Average CN				
	NBO	ВО	TBO	Q_2	Q_3	Q_4	Q_5	Q_2	Q_3	Q_4	(%)	В	Si	Na
Original	1.1	98.4	0.5	0.1	2.4	97.5		1.2	70.9	27.9	28.0	3.26	4.00	6.73
Pressure quenched	0.7	96.3	3.0		1.3	98.5	0.2	1.0	60.9	38.1	38.3	3.38	4.00	8.91
Pressure- RT	1.1	97.4	1.5	0.1	2.3	97.6		1.3	67.3	31.4	31.6	3.31	4.00	7.32
Annealed	1.2	97.9	0.9		2.5	97.5		1.8	69.5	28.7	28.8	3.29	4.00	7.15

Table 2 summarizes the short range structural details of the pressure quenched samples: oxygen speciation, Q_n speciation of B and Si, and average coordination numbers of all the cations. There exist three types of oxygen species in these glasses: non-bridging oxygen (NBO), bridging oxygen (BO) and three-bonded oxygen (TBO), which is defined as oxygen atom connected to one, two, and three glass former cations (Si or B), respectively. For all of these samples, over 96% of oxygen are BOs forming the dominating oxygen species and suggesting the glass structure is made up of three dimensional network made up of [SiO₄], [BO₃], [BO₄] polyhedra linked through cornersharing of common oxygen. As compared to the original glass, the percentage of TBO for pressure quenched glass (Fig. 5 (b)) increased from 0.5% to 3%, and the percentage of NBO and BO concentration decreased accordingly. The average coordination number of boron increased from 3.26 to 3.38 due to an 18% increase of four-fold coordinated boron, while silicon remain perfectly four-fold coordinated. The only exception is the hot pressure quenched sample has about 0.2% 5fold coordinated Si when pressure quenched under 10 GPa. Notably, the coordination number of sodium also increased significantly from 6.7 to 8.9, an increase of 33%, after pressure quenching. After annealing, the coordination number for Na decreased to 7.15, but still higher than the original value (6.73). These analyses suggest the pressure quench process mainly led to the structural changes around boron and sodium but left the silica network more or less unchanged.

The cation (Si and B) environment around oxygen species NBO, BO and TBO were further analyzed and the results are shown in Fig. 5. It can be seen that there is a decrease of NBO in the pressure quenched sample (Fig. 5 (a)) but the decrease is much larger for those NBO bonded to Si than those bonded to B. The most obvious change is on TBO after the pressure treatment. Not only the percentage of TBO increased from 0.7 to 3% in the pressure quenched sample, the types of cations linked to TBO are also different. For the original and annealed samples, all TBOs are connected at least to one boron: 3B, 2B1Si or 1B2Si. While for the pressure quenched and Pressure-RT samples, we can notice the emergence of TBO connected to three silicon. This type of TBOs is unexpected and was not observed in glasses in room temperature. As the five-fold coordinate silicon only exist in pressure quenched sample, this type of TBO might be related to distortion of silicon oxygen tetrahedra under pressure. Fig. 5 (c) shows the types of glass former cations linkages through common bridging oxygen. While the three types of linkages remain largely unchanged in the samples, the [SiO4]-[SiO4] connection of pressure quenched glass showed a slight decrease as compared to the original glass.

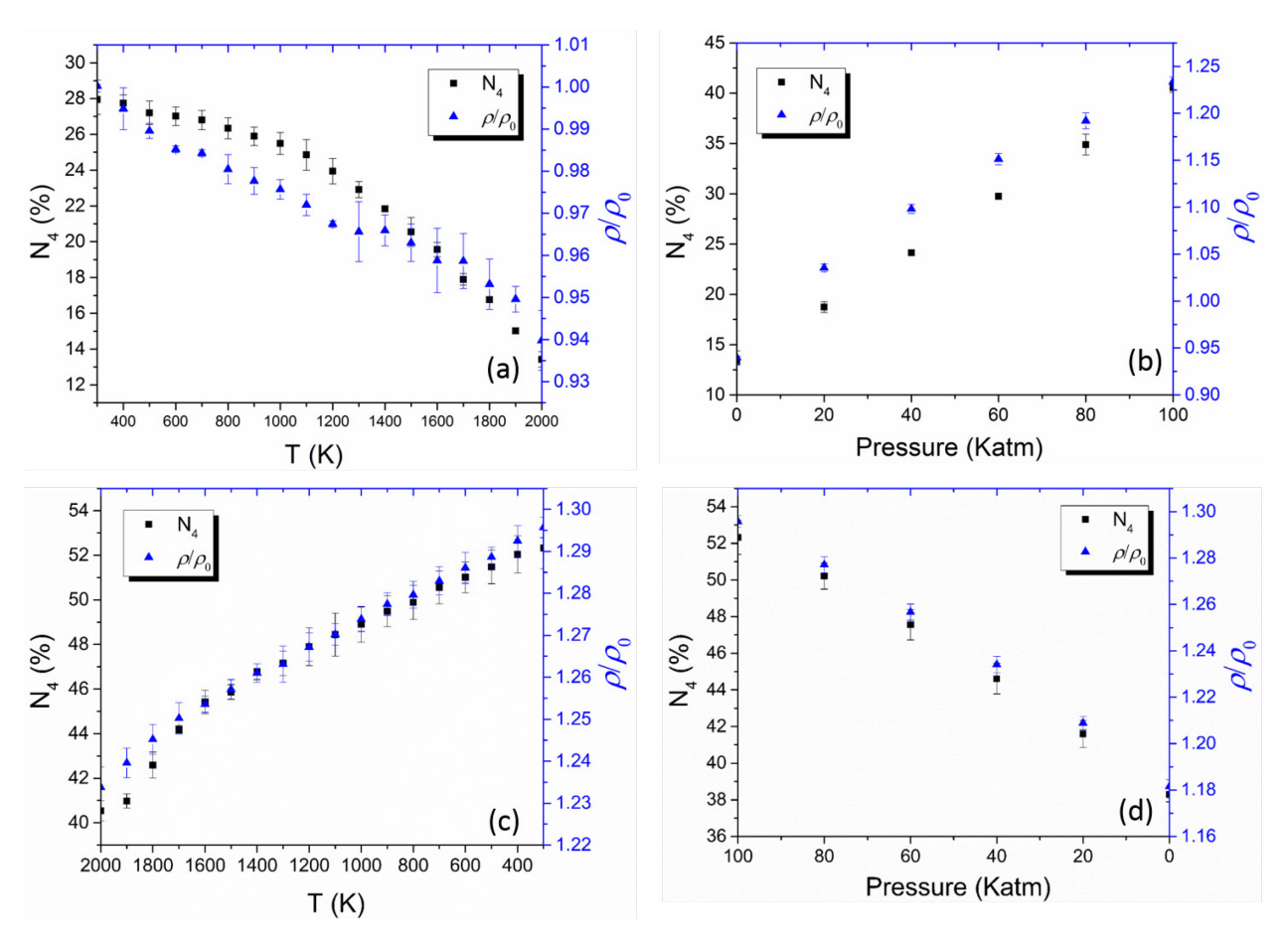


Fig. 4. Boron N_4 and glass density change (ρ_0 is the density of original glass) in the pressure quenching process. (a) heating at room pressure, (b) increase pressure at 2000 K, (c) cooling at 10 GPa, (d) decrease pressure at room temperature (300K).

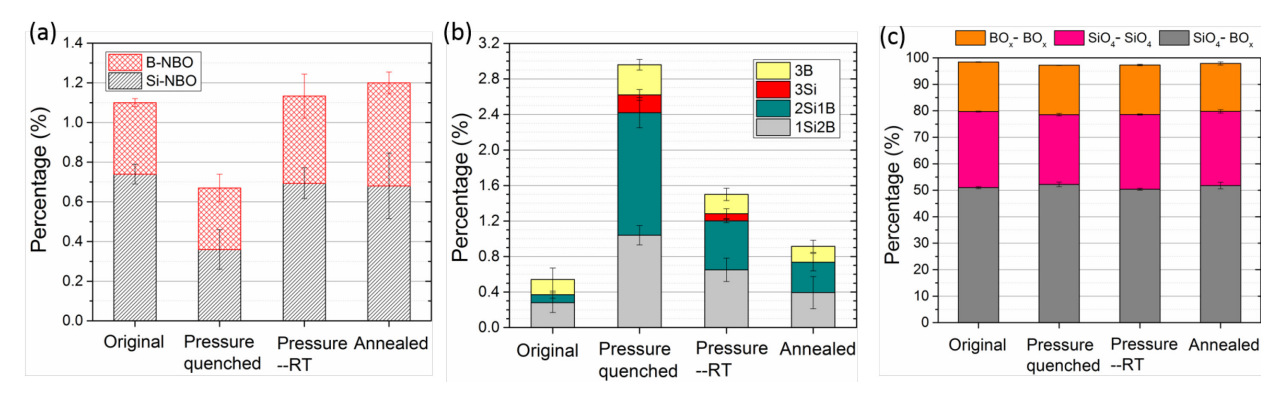


Fig. 5 Oxygen speciation in the borosilicate glasses under pressure quenching and annealing. (a) percentage of non-bridging oxygen (NBO) around silicon and boron, (b) percentage and type of three-bonded oxygen (TBO), (c) glass former oxygen polyhedron connection percentages

Q_n (glass-former atom connecting with *n* bridging oxygen) species distributions for Si and B were analyzed and are also shown in Table 2. More than 97% of Si in all these glasses are Q₄ species. After pressure quench, Si-Q₄ increased from 97.5% to 98.5%, and the new formed 0.2 % ^[5]Si are in Q₅ species. Considering the fact that the difference between B N₄ and Q₄ for all these samples are around 2%, it can be known that most of four-coordinated boron ^[4]B are bonded with four BOs. Similarly, most ^[3]B in these glass structures are in Q₃ species and there are around 1-2% ^[3]B that connected to one NBO.

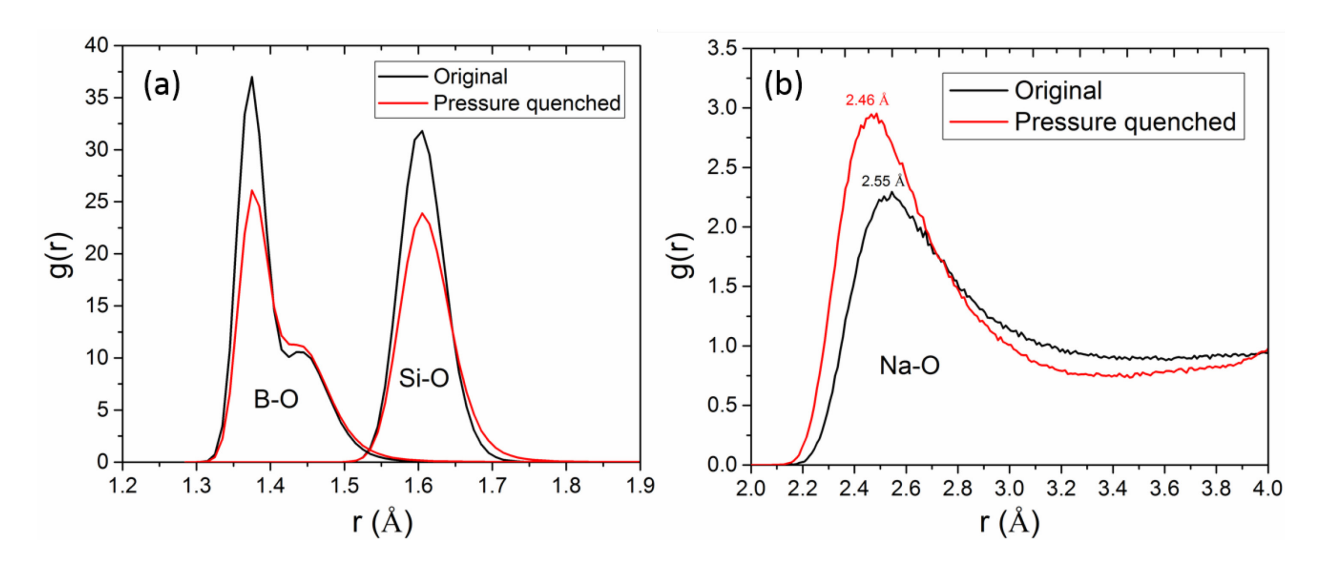


Fig. 6 Comparison of original and pressure quenched glass PDF for (a) B-O and Si-O (b) Na-O

Cation-oxygen pair distribution function (PDF) (Fig. 6) before and after pressure quench provide direct information of coordination environment change of the cations. As compared with the original glass, the Si-O for pressure quenched glass are broader with larger FWHM (full width at half maximum) and show a shoulder on the longer distance side, indicating a wider distribution of Si-O bond length and increase of Si-O bonds with longer bond length. For B-O PDF, the first and second peak around 1.37 Å and 1.45 Å was attributed to [3]B-O and [4]B-O respectively, which is in good agreement with pervious experimental and simulation results [16, 26, 27]. A more remarkable change comes from the Na-O PDF, in which the Na-O first peak becomes more intense and the peak position shift to a shorter distance from 2.55 Å to 2.46 Å, indicating a significant

decrease of average Na-O bond length and increase of order around sodium ions after the pressure quench treatment.

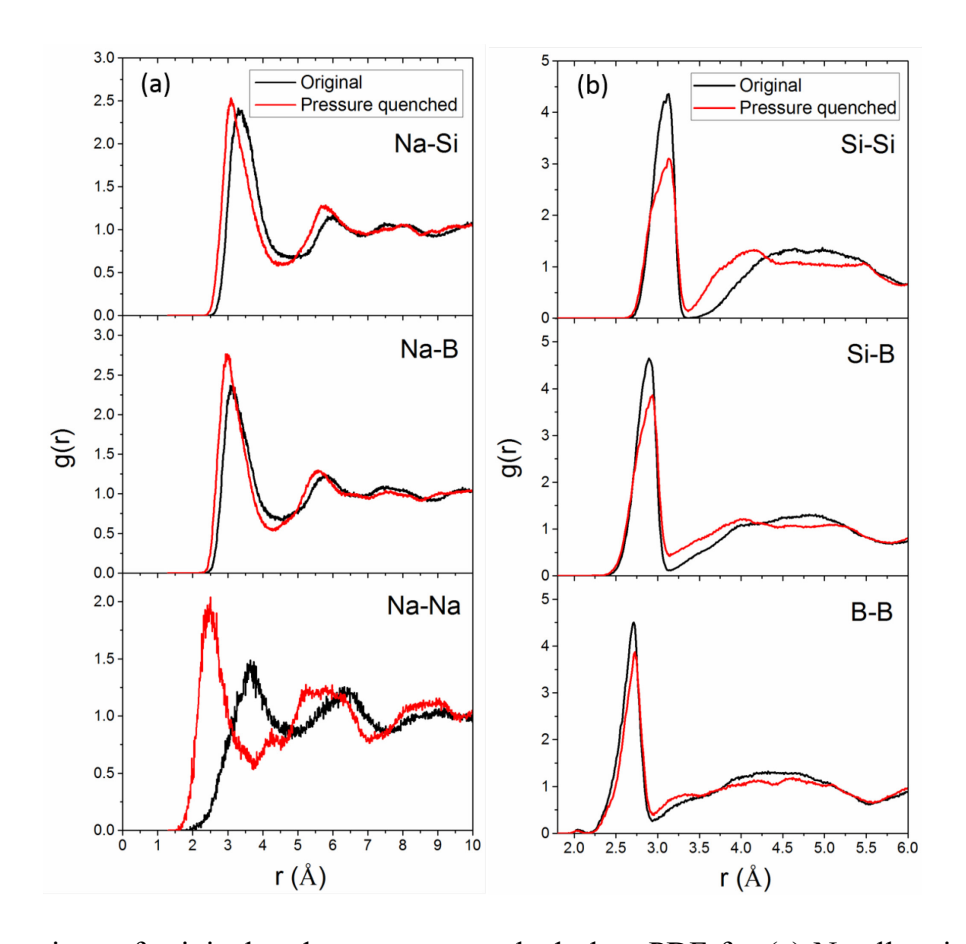


Fig. 7 Comparison of original and pressure quenched glass PDF for (a) Na-all cation (b) glass former cation-cation

Cation-cation pair distribution function provide medium range structure information of distribution and correlation of the glass former and modifier cations. Fig. 7(a) shows the Na involved PDFs: Na-Si, Na-B and Na-Na. The first peak for these three PDFs shifted to lower distance and the peak height increased after pressure quench process. Among all the changes, the one for Na-Na is most notable. The average Na-Na first neighbor distance changed drastically from 3.75 Å to 2.50 Å, suggesting there is an increased level of sodium segregation in pressured quenched sample. Together with increased Na coordination number, our simulation results suggest that pressure quench effect has strong impact in the sodium rich regions. Based on the modified random network model²⁴, the modifier and NBO rich regions are more prone to the pressure than the network regions. Fig. 7(b) shows the PDF between glass formers. It can be seen that there is

almost no change of first peak positions for all these PDFs. But there is a left shift of second peak, especially for Si-Si PDF, indicating the decrease of second shell coordination atom distance.

The short and medium structures around sodium were further analyzed by calculating Na-O and Na-Na/B/Si total correlation functions and accumulated coordination numbers (Fig. 8). The Na-O, Na-Na, Si-Na, and B-Na first peak all shifted to shorted bond distances and had increased intensity, which suggest increase of oxygen coordination number around Na and Na coordination number around Na, B and Si in pressure quenched samples.

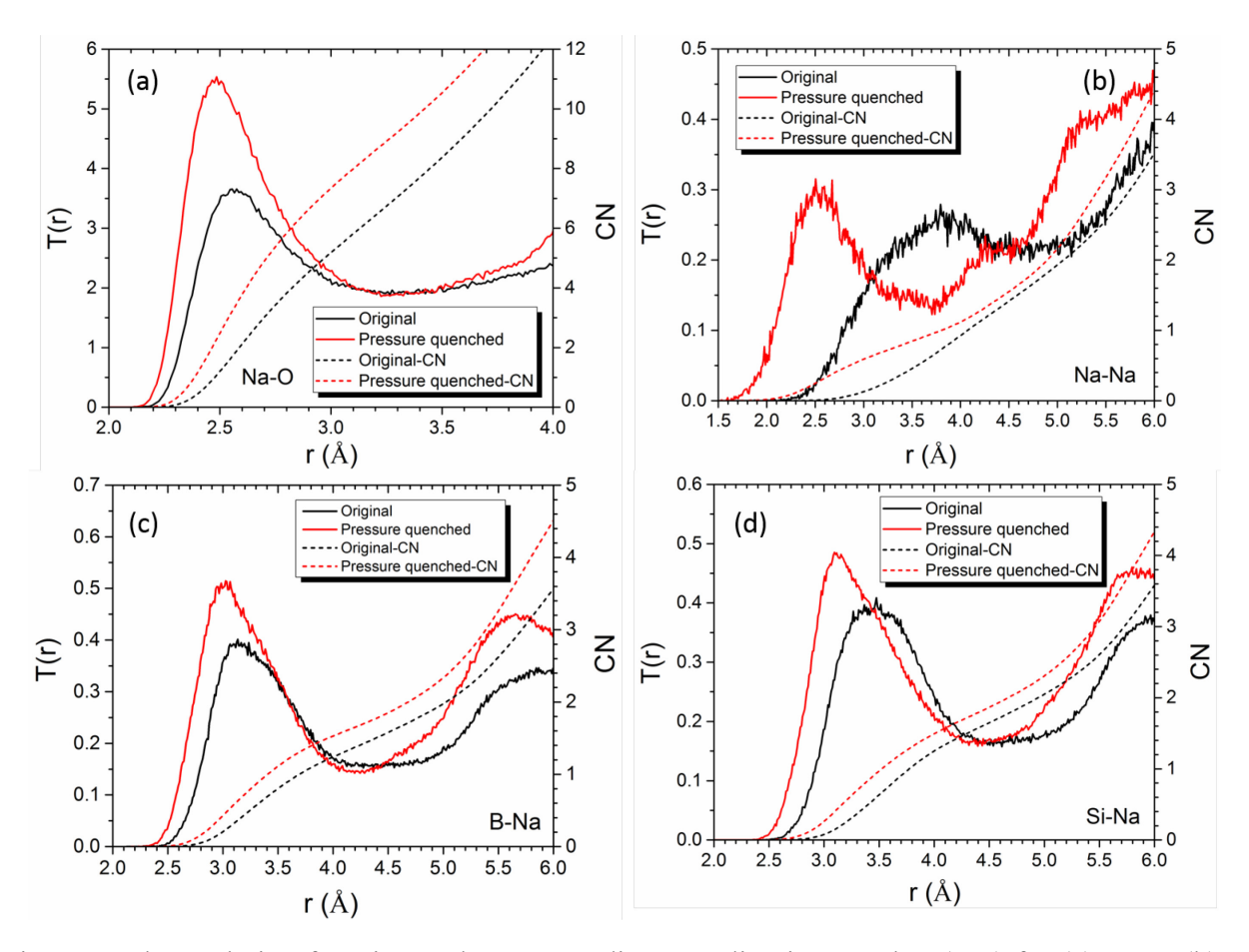


Fig. 8 Total correlation function and corresponding coordination number (CN) for (a) Na-O (b) Na-Na (c)B-Na (d)Si-Na in as formed and pressured quenched NBS glasses

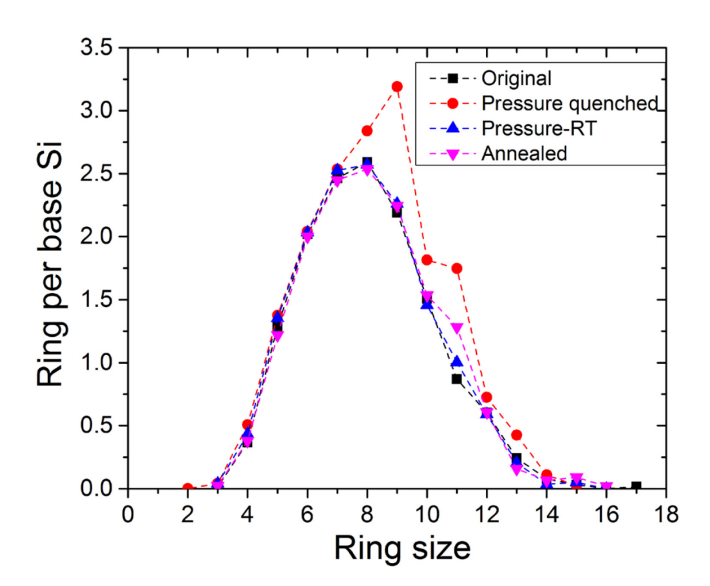


Fig. 9 Primitive ring distribution of the glass forming network for pressure quenched and annealed glasses as compared to the original glass

For medium range structure characterization, primitive ring size distribution was calculated and shown in Fig. 9. The primitive ring here are defined as the smallest closed chain formed by bridging oxygen and glass formers (Si and B). A size of N-membered ring means the total number of network formers in the primitive ring equals N. From Fig. 9 it can be seen that the ring size distribution for Pressure-RT and Annealed samples are quite similar to the one for original glass. These three ring size distributions show a relatively symmetric Gaussian type distribution ranging from 3 to 16, with a peak at 8. As for the pressure quenched sample, there is an increase of higher ring size (> 8) and the peak position shifted to 9. The increase in number of larger rings has been confirmed by several MD simulation studies on pressure-induced change of ring statistics in silica glass. 10, 25 Previous first principles and classical MD simulation found that 6-membered rings are the most abundant in pristine silica glass. Huang et al. [31] reported that pressurization caused an increase in number of larger rings of silica glass at the expense of smaller rings. In another MD simulation of fused silica under high pressure, a decrease of 5, 6-membered ring, an increase of 3, 4-membered rings as well as larger rings (> 7) have been deduced [32]. For this SBN glass, the change of smaller rings (< 8) was not observed (Fig. 9). The increase of larger rings for pressure quenched glass can be related to the increase of B N₄, since 4-fold coordinated boron preferred to be linked with [SiO₄] tetrahedra in the glass former network [33].

3.3 Effect of pressure and thermal history on glass properties

To understand the effect of pressure quenching on the mechanical properties of glasses, the Bulk (B), Shear (G) and Young's moduli (E) for the four samples under different pressure quenching procedures were calculated and the results are shown in Table 3. The method used for mechanical property calculation has been elaborated in our previous work [18]. It can be seen that the as-melted (original) and pressure quenched glass have the lowest and highest elastic moduli respectively, with the moduli for Pressure-RT and Annealed samples line in between. The increase of Young's moduli is quite dramatic: that of 80.5 GPa for the as formed glass was increased by 90% to 152.8 GPa for the pressure quenched sample. In comparison, the room temperature pressured sample has an increase by 18% and the annealed sample has an increase by 11% as compared to the as formed glass. The bulk and shear moduli also show similar increase in the pressure quenched sample. Elastic moduli are mostly related to two factors: the interatomic bonding strength and atomic packing factor [34]. As there is no glass composition change in this work, the increase of elastic moduli for pressure quench sample should mainly due to a denser packing state. By calculating the final glass density for different samples, we can see that the glass density and elastic moduli are positively related to each other, with both of them decreasing in the following sequence: Pressure quenched > Pressure-RT > Annealed > As-melted.

Table 3 Mechanical properties (bulk modulus B, Young's modulus E, Shear modulus G) as a function of the pressure and annealing process

		Density (g/cm ³)		
	В	G	Е	,
As-melted	38.7 ± 0.6	34.9 ± 0.3	80.5 ± 0.6	2.41
Pressure quenched	83.5 ± 2.1	64.0 ± 0.2	152.8 ± 0.7	2.85
Pressure-RT	45.8 ± 3.6	41.0 ± 2.0	94.7 ± 5.3	2.56
Annealed	45.9 ± 1.2	38.1 ± 0.6	89.5 ± 0.9	2.51

4. Discussion

Borosilicate glass is an important glass family that find wide industrial applications from display, nuclear waste disposal, pharmaceutical to fiber glasses [35]. The properties of borosilicate glasses are commonly modified by changing the composition and thermal history. Pressure has been used as an additional tool to change the properties of borosilicate glasses due to the relatively easy change of boron coordination under pressure [1,2,36–39]. Our simulation results show that hot compression at a temperature close to Tg and pressure up to 10 GPa led to significant property changes as summarized in Fig. 10. The elastic moduli increased by 90%, shear moduli by 83% and bulk modulus by 115% in hot compressed sample as compared to the as melted glass. Cold compressed sample also has higher moduli but the increase is much smaller: around 18% for all three moduli. Annealing at ambient pressure and Tg led to recovery of the moduli to values close to cold compressed samples, still 10-18% higher than the as-melted glass. These results are consistent with experimental observations: a recent study by Wu et al. found that hot compression in calcium boroaluminosilciate glasses led to 13 to 41% increase of Young's modulus when the pressure is 2 GPa [9]. The increase of moduli and pressure derivation of moduli increases are larger for glasses with higher amount of boron oxide [9]. Bulk and Shear moduli showed similar changes.

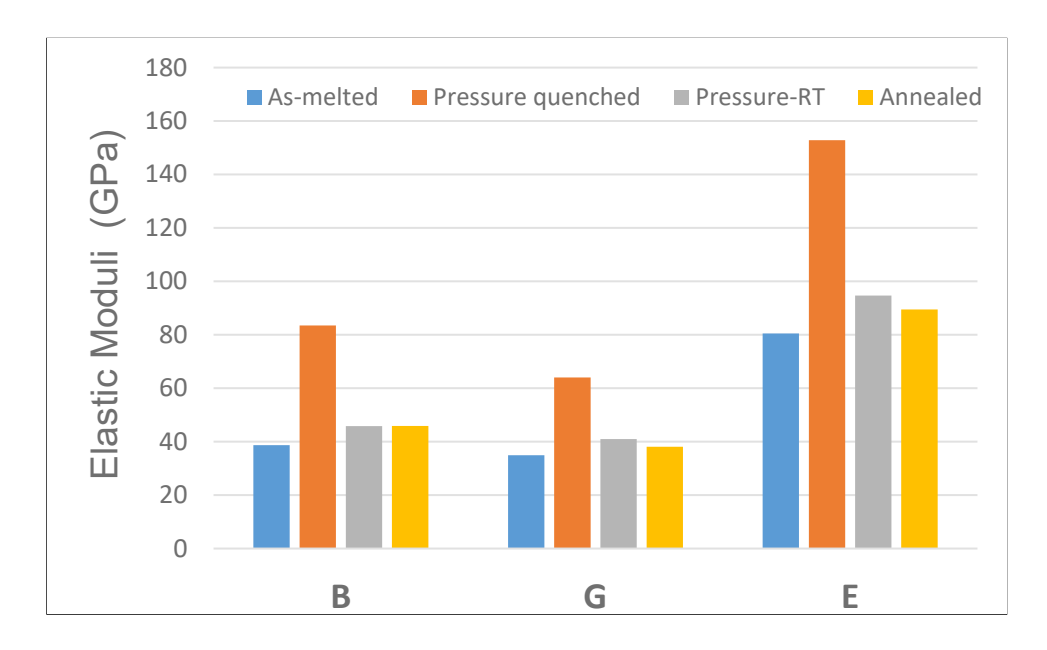


Fig. 10 Elastic moduli changes with different pressure processing conditions. Bulk modulus B, Young's modulus E, Shear modulus G. Pressure quenched: hot compression at T_g and 10 GPa, pressure-RT: cold compression at room temperature, Annealed: annealing at ambient pressure at around Tg.

After compression, most of the Si atoms in borosilicate glasses still maintain tetrahedral coordination while boron shows an obvious increase of coordination. Pressure-induced ^[3]B to ^[4]B transition has been confirmed by several experimental researches ranging from pure B₂O₃ glass to various boron containing glass [37–40]. Du et al. [33] studied the pressure-induced structural changes using high-resolution ¹¹B and ¹⁷O NMR on a SBN glass (R=1.06, K=2) melt at 5 GPa. They proposed that the pressure-induced change of boron coordination is related to the presence of NBO in the glass through the following reaction:

$$^{[3]}B + NBO \rightarrow ^{[4]}B \tag{2}$$

This was regarded as the energetically "easy" pathway for boron coordination increases. However, in the case of the sodium borosilicate glass investigated in this work (with R=0.3 and K=2), due to the low concentration of Na₂O, there is only 1.1 % NBO in the original glass (Table 2). As shown in Table 2, after the pressure quench process, the fraction of NBO further dropped by 0.4 % (from 1.1% to 0.7%) while the TBO in the glass structure increased from 0.5% to 3.0%. These results suggest that there might exist a different mechanism to explain the boron coordination increase in this SBN glass with relatively low sodium concentration [40]:

$$^{[3]}B + BO \Rightarrow ^{[4]}B + TBO \tag{3}$$

The increase of TBO concentration and decrease of BO concentration (Table 2) after pressure quenching strongly supports this mechanism. However, as the glass composition studied in this work represents those with low soda content, as reflected in low R value (0.3), more studies on wider composition ranges would be needed to further confirm this mechanism.

In addition to the coordination number change around boron, sodium as a glass modifier ion also plays an important role during pressure quenching. Based on our MD simulation results, there was around 3.7% decrease of Na-O bond length and around 33% increase of the average oxygen coordination number around sodium: from 6.7 to 8.9 after pressure-quench. In addition, the average first neighbor distance for Na-Na decreased from 3.75 Å to 2.50 Å after compression (corresponds to a ~33% shrink), indicating an increased level of segregation of Na ions in the pressure quenched glass structure. These dramatic environment changes around Na⁺ show that the decrease of sodium ion free volume plays an important role in the densification mechanism for this SBN glass. The decrease of Na-O distance after compression has been confirmed by several

experimental researches for various glasses [6,39,41]. For example, Wu et al. studied the pressure-quench effect on aluminoborosilicate melts of the E-glass composition [39]. With the help of ²³Na NMR, they found a 0.7% shortening of mean Na-O from ambient pressure to 500 MPa and pointed out that the compression of the network modifier cation volumes was important for the glass densification. However, it is still impossible experimentally to resolve different coordination numbers or neighbor types (BO and NBO) from ²³Na MAS spectra [39]. In general, pressure-induced coordination transformation of modifier ions is more difficult to characterize than the glass former cations. Lee et al. studied the first inelastic x-ray scattering (IXS) Li *K*-edge spectra for Li₂B₄O₇ glasses and found that the Li ion K-edge spectra up to 5 GPa show little difference as compared to that at 1 atm [42]. It was pointed out that these results are considered preliminary so further theoretical and experimental studies are still required to reveal pressure-induced coordination changes of the glass modifiers [42].

Based on the modified random network (MRN) [38, 39] model of silicate glasses, the glass structure consists of the glass former network rich regions linked by modifier and NBO rich regions. The MRN model was supported by MD simulations of alkali silicate glasses [44,45]. Under external pressure, both regions are compressed but the stress experienced by the two can be different due to bonding strength and structural differences. Our simulation results show that the pressure quenching lead to an increase of boron coordination, which reflects the effect of pressure on the glass former rich regions, and an increase of sodium coordination number, which represents the pressure effect on the modifier/NBO rich regions. From the percentage change of coordination of the two: 18% and 33% for B and Na respectively, it can be concluded that the compression on the modifier/NBO rich regions is larger. This is further supported by dramatic decrease of Na-Na average distances and shift of first peak of Na-Na PDF.

The annealing effect on pressure-quenched sample and cold compression (compressed at room temperature) effect on original SBN glass were also investigated in this work. The results provide useful information to understand the effect of pressure quenching on the structure and properties. After annealing, both pressure-induced macroscopic properties (i.e. density and elastic moduli) and microstructural features (such as CN for B³⁺ and Na⁺) show a large extent of relaxation. A recent experimental research on pressure induced structural change of a soda-lime borate glass (25Na₂O-10CaO-65B₂O₃, in mol%) also reported the relaxation of macroscopic properties after

annealing at 0.9 Tg [38]. But it was found that the pressure-induced coordination change of boron remains unchanged upon annealing [38]. In our simulations, boron coordination decreased to 3.29 in annealed sample from 3.38 in the pressure quenched sample. This difference might be due to glass composition difference: our simulation is on a borosilicate glass while the experimental work was done on a pure borate glass [38]. As compared to hot compression or pressure quenching, it is well accepted that cold compression is much less effective and much higher pressure (usually above 8-10 GPa) is required to achieve permanent densification of a glass. Our simulation results are consistent with this observation. With the same compression pressure (10 GPa) and duration (2 ns) for cold compression and pressure quench, the degree of densification in cold compressed glass is much lower than pressure-quenched glass. The annealing at glass transition temperature and ambient pressure removed most of the pressure effect. As a result, the density of cold compressed sample is slightly higher than the annealed sample. Our results thus show that our MD simulations are able to reproduce most of the pressure induced effects in borosilicate glasses under hot compression, cold compression and annealing. Detailed short and medium range structure features are obtained to explain the structural origins of the associated property changes. Further investigation of the composition (e.g. boron oxide concentration or R and K values) and compression temperature effects on the structural and property changes during hot compression would be highly valuable.

It is worth pointing out that our results show evidence of pressure quenching at a temperature close to T_g led to permanent densification and large property changes, while applying pressure at ambient temperature does not. Experimentally it was found that permanent densification can happen at a temperature close to 0.9 T_g [38]. An interesting question of technical importance is what is the lowest temperature at which a permanent densification can happen. This requires a systematic study of pressure quenching with gradually increasing temperatures and will be reported in a subsequent paper.

5. Conclusions

Structure changes due to pressure quenching in a sodium borosilicate glasses (R=0.3, K=2) were investigated by using constant pressure molecular dynamics simulations with recently developed potentials. The densification mechanism was found to originate mainly from the local

environment change of boron and sodium: there are notable increase of coordination number for both B and Na, by 18% and 33% respectively, while the coordination number of Si remains unchanged in the process. Furthermore, a decrease of average Na-O and Na-Na bond distance was also observed, suggesting compression has a large effect on the sodium and NBO rich regions in the picture of structural heterogeneity described by the modified random network model. Interesting change in the medium-range order was also observe. In addition, a direct correlation between boron N₄ value and oxygen triculster (one oxygen bond to three glass former cations) was observed, suggesting the latter as an additional charge compensation mechanism for [BO₄] unit in pressure quenched samples where experience sodium depletion due to increased sodium ion segregation. Medium range structures was also modified due to hot compression and there is clear increase of concentration of larger rings with size 8 higher in the pressure quenched sample. Pressure quenched glass was found to increase the mechanical properties, almost doubling the elastic moduli of the initial glass. The effects of annealing and cold compression were also investigated to compare the pressure quenching with temperature. Our simulation results show that the level of glass densification decrease in the sequence: Pressure quenched >> Cold compression (Pressure-RT) > Annealed. The results show that MD simulations with effective potentials can be a very valuable tool in investigating pressure quenching induced structural and property changes in network forming oxide glasses.

Acknowledgement:

The authors gratefully acknowledge financial support by US National Science Foundation (project # 1662288).

References:

- [1] S. Kapoor, L. Wondraczek, M.M. Smedskjaer, Pressure-induced densification of oxide glasses at the glass transition, Front. Mater. 4 (2017) 1–20. https://doi.org/10.3389/fmats.2017.00001.
- [2] T. Du, S.S. Sørensen, T. To, M.M. Smedskjaer, Oxide glasses under pressure: Recent insights from experiments and simulations, J. Appl. Phys. 131 (2022). https://doi.org/10.1063/5.0088606.
- [3] A.K. Varshneya, Fundamentals of inorganic glasses, Society of Glass Technology, 2013.

- [4] M.N. Svenson, G.L. Paraschiv, F. Mu??oz, Y. Yue, S.J. Rzoska, M. Bockowski, L.R. Jensen, M.M. Smedskjaer, Pressure-induced structural transformations in phosphorus oxynitride glasses, J. Non. Cryst. Solids. 452 (2016) 153–160. https://doi.org/10.1016/j.jnoncrysol.2016.08.039.
- [5] M.N. Svenson, R.E. Youngman, Y. Yue, S.J. Rzoska, M. Bockowski, L.R. Jensen, M.M. Smedskjaer, Volume and Structure Relaxation in Compressed Sodium Borate Glass, Phys. Chem. Chem. Phys. Phys. Chem. Chem. Phys. Accept. Manuscr. 18 (2016) 29879–29891. https://doi.org/10.1039/C6CP06341A.
- [6] M.N. Svenson, L.M. Thirion, R.E. Youngman, J.C. Mauro, S.J. Rzoska, M. Bockowski, M.M. Smedskjaer, Pressure-induced changes in interdiffusivity and compressive stress in chemically strengthened glass, ACS Appl. Mater. Interfaces. 6 (2014) 10436–10444. https://doi.org/10.1021/am5019868.
- [7] S.K. Lee, Y.H. Kim, P. Chow, Y. Xiao, C. Ji, G. Shen, Amorphous boron oxide at megabar pressures via inelastic X-ray scattering, Proc. Natl. Acad. Sci. U. S. A. 115 (2018) 5855–5860. https://doi.org/10.1073/pnas.1800777115.
- [8] S. Bista, J.F. Stebbins, J. Wu, T.M. Gross, Structural changes in calcium aluminoborosilicate glasses recovered from pressures of 1.5 to 3 GPa: Interactions of two network species with coordination number increases, J. Non. Cryst. Solids. 478 (2017) 50–57. https://doi.org/10.1016/j.jnoncrysol.2017.09.053.
- [9] J. Wu, T.M. Gross, L. Huang, S.P. Jaccani, R.E. Youngman, S.J. Rzoska, M. Bockowski, S. Bista, J.F. Stebbins, M.M. Smedskjaer, Composition and pressure effects on the structure, elastic properties and hardness of aluminoborosilicate glass, J. Non. Cryst. Solids. 530 (2020) 119797. https://doi.org/10.1016/j.jnoncrysol.2019.119797.
- [10] J. Du, A. N. Cormack, eds., Atomistic Simulations of Glasses Fundamentals and Applications, Wiley, 2022. https://doi.org/10.1002/9781118939079.
- [11] J. Du, Molecular Dynamics Simulations of Oxide Glasses, in: L. Musgraves, J. David; Hu, Junjie; Calvez (Ed.), Springer Handb. Glas., 2019: pp. 1131–1155. https://doi.org/10.1007/978-3-319-93728-1_32.
- [12] L. Deng, J. Du, Borosilicate and Boroaluminosilicate Glasses, in: At. Simulations Glas., Wiley, 2022: pp. 224–260. https://doi.org/10.1002/9781118939079.ch8.
- [13] L. Deng, J. Du, Erratum: Development of boron oxide potentials for computer simulations of multicomponent oxide glasses (Journal of the American Ceramic Society, (2019), 102, 5, (2482-2505), 10.1111/jace.16082), J. Am. Ceram. Soc. 103 (2020). https://doi.org/10.1111/jace.16897.
- [14] S. Sundararaman, L. Huang, S. Ispas, W. Kob, New interaction potentials for borate glasses with mixed network formers, (n.d.) 1–22.
- [15] M. Wang, N.M. Anoop Krishnan, B. Wang, M.M. Smedskjaer, J.C. Mauro, M. Bauchy, A new transferable interatomic potential for molecular dynamics simulations of borosilicate glasses, J. Non. Cryst. Solids. 498 (2018) 294–304. https://doi.org/10.1016/j.jnoncrysol.2018.04.063.

- [16] B. Stevensson, Y. Yu, M. Edén, Structure-composition trends in multicomponent borosilicate-based glasses deduced from molecular dynamics simulations with improved B-O and P-O force fields, Phys. Chem. Chem. Phys. 20 (2018) 8192–8209. https://doi.org/10.1039/c7cp08593a.
- [17] L.-H. Kieu, J.-M. Delaye, L. Cormier, C. Stolz, Development of empirical potentials for sodium borosilicate glass systems, J. Non. Cryst. Solids. 357 (2011) 3313–3321.
- [18] L. Deng, J. Du, Development of effective empirical potentials for molecular dynamics simulations of the structures and properties of boroaluminosilicate glasses, J. Non. Cryst. Solids. 453 (2016) 177–194. https://doi.org/10.1016/j.jnoncrysol.2016.09.021.
- [19] W.J. Dell, P.J. Bray, S.Z. Xiao, 11B NMR studies and structural modeling of Na2OB2O3SiO2 glasses of high soda content, J. Non. Cryst. Solids. 58 (1983) 1–16. https://doi.org/10.1016/0022-3093(83)90097-2.
- [20] D.A. Kilymis, J.-M. Delaye, S. Ispas, Behavior of sodium borosilicate glasses under compression using molecular dynamics., J. Chem. Phys. 143 (2015) 094503. https://doi.org/10.1063/1.4929785.
- [21] L. Ding, K.H. Lee, T. Zhao, Y. Yang, M. Bockowski, B. Ziebarth, Q. Wang, J. Ren, M.M. Smedskjaer, J.C. Mauro, Atomic structure of hot compressed borosilicate glasses, J. Am. Ceram. Soc. 103 (2020) 6215–6225. https://doi.org/10.1111/jace.17377.
- [22] K.H. Lee, Y. Yang, L. Ding, B. Ziebarth, M.J. Davis, J.C. Mauro, Plasticity of borosilicate glasses under uniaxial tension, J. Am. Ceram. Soc. 103 (2020) 4295–4303. https://doi.org/10.1111/jace.17163.
- [23] L. Deng, J. Du, Development of boron oxide potentials for computer simulations of multicomponent oxide glasses, J. Am. Ceram. Soc. 102 (2019) 2482–2505.
- [24] W. Smith, T. Forester, DL_POLY_2. 0: A general-purpose parallel molecular dynamics simulation package, J. Mol. Graph. 14 (1996) 136–141.
- [25] B. Guillot, N. Sator, A computer simulation study of natural silicate melts. Part II: High pressure properties, Geochim. Cosmochim. Acta. 71 (2007) 4538–4556.
- [26] L.H. Kieu, J.M. Delaye, L. Cormier, C. Stolz, Development of empirical potentials for sodium borosilicate glass systems, J. Non. Cryst. Solids. 357 (2011) 3313–3321. https://doi.org/10.1016/j.jnoncrysol.2011.05.024.
- [27] K. Takahashi, A. Osaka, R. Furuno, The elastic properties of the glasses in the systems R2O-boron oxide-silicon dioxide (R= sodium and potassium) and sodium oxide-boron oxide., Yogyo Kyokaishi. 91 (1983) 199–205.
- [28] A. Grandjean, M. Malki, C. Simonnet, Effect of composition on ionic transport in SiO2-B2O3-Na2O glasses, J. Non. Cryst. Solids. 352 (2006) 2731–2736. https://doi.org/10.1016/j.jnoncrysol.2006.03.058.
- [29] M. Ren, L. Deng, J. Du, Bulk, surface structures and properties of sodium borosilicate and boroaluminosilicate nuclear waste glasses from molecular dynamics simulations, J. Non. Cryst. Solids. 476 (2017) 87–94. https://doi.org/10.1016/j.jnoncrysol.2017.09.030.

- [30] R.L. Mozzi, B.E. Warren, The structure of vitreous boron oxide, J. Appl. Crystallogr. 3 (1970) 251–257. https://doi.org/10.1107/s0021889870006143.
- [31] L. Huang, J. Kieffer, Thermomechanical anomalies and polyamorphism in B2 O3 glass: A molecular dynamics simulation study, Phys. Rev. B Condens. Matter Mater. Phys. 74 (2006) 1–10. https://doi.org/10.1103/PhysRevB.74.224107.
- [32] L.P. Dávila, M.J. Caturla, A. Kubota, B. Sadigh, T. Díaz de la Rubia, J.F. Shackelford, S.H. Risbud, S.H. Garofalini, Transformations in the medium-range order of fused silica under high pressure, Phys. Rev. Lett. 91 (2003) 1–4. https://doi.org/10.1103/PhysRevLett.91.205501.
- [33] L.S. Du, J.R. Allwardt, B.C. Schmidt, J.F. Stebbins, Pressure-induced structural changes in a borosilicate glass-forming liquid: Boron coordination, non-bridging oxygens, and network ordering, J. Non. Cryst. Solids. 337 (2004) 196–200. https://doi.org/10.1016/j.jnoncrysol.2004.03.115.
- [34] N. Soga, Elastic moduli and fracture toughness of glass, J. Non. Cryst. Solids. 73 (1985) 305–313. https://doi.org/10.1016/0022-3093(85)90356-4.
- [35] Y. Yue, M.I. Tuheen, J. Du, Borosilicate Glasses, in: M. Pomeroy (Ed.), Encycl. Mater. Ceram. Glas., Elsevier, 2021: pp. 519–539. https://doi.org/10.1016/B978-0-12-818542-1.00098-9.
- [36] M.F. Hochella, G.E. Brown, The structures of albite and jadeite composition glasses quenched from high pressure, Geochim. Cosmochim. Acta. 49 (1985) 1137–1142. https://doi.org/10.1016/0016-7037(85)90004-3.
- [37] S. Kapoor, X. Guo, R.E. Youngman, C.L. Hogue, J.C. Mauro, S.J. Rzoska, M. Bockowski, L.R. Jensen, M.M. Smedskjaer, Network Glasses under Pressure: Permanent Densification in Modifier-Free Al2 O3- B2 O3- P2 O5-SiO2 Systems, Phys. Rev. Appl. 7 (2017) 1–16. https://doi.org/10.1103/PhysRevApplied.7.054011.
- [38] M.M. Smedskjaer, R.E. Youngman, S. Striepe, M. Potuzak, U. Bauer, J. Deubener, H. Behrens, J.C. Mauro, Y. Yue, Irreversibility of pressure induced boron speciation change in glass, Sci. Rep. 4 (2014) 1–6. https://doi.org/10.1038/srep03770.
- [39] J. Wu, J. Deubener, J.F. Stebbins, L. Grygarova, H. Behrens, L. Wondraczek, Y. Yue, Structural response of a highly viscous aluminoborosilicate melt to isotropic and anisotropic compressions, J. Chem. Phys. 131 (2009). https://doi.org/10.1063/1.3223282.
- [40] S.K. Lee, P.J. Eng, H.K. Mao, Y. Meng, M. Newville, M.Y. Hu, J. Shu, Probing of bonding changes in B2O3 glasses at high pressure with inelastic X-ray scattering, Nat. Mater. 4 (2005) 851–854. https://doi.org/10.1038/nmat1511.
- [41] J.R. Allwardt, J.F. Stebbins, B.C. Schmidt, D.J. Frost, A.C. Withers, M.M. Hirschmann, Aluminum coordination and the densification of high-pressure aluminosilicate glasses, Am. Mineral. 90 (2005) 1218–1222. https://doi.org/10.2138/am.2005.1836.
- [42] S.K. Lee, P.J. Eng, H.K. Mao, Y. Meng, J. Shu, Structure of alkali borate glasses at high pressure: B and Li K-edge inelastic X-ray scattering study, Phys. Rev. Lett. 98 (2007) 1–4. https://doi.org/10.1103/PhysRevLett.98.105502.

- [43] G.N. Greaves, Exafs and the structure of glass g.n. greaves, J. Non. Cryst. Solids. 71 (1985) 203–217.
- [44] T. Mahadevan, J. Du, Silica, Silicate, and Aluminosilicate Glasses, in: At. Simulations Glas., Wiley, 2022: pp. 186–223. https://doi.org/10.1002/9781118939079.ch7.
- [45] J. Du, A.N. Cormack, The medium range structure of sodium silicate glasses: A molecular dynamics simulation, J. Non. Cryst. Solids. 349 (2004) 66–79. https://doi.org/10.1016/j.jnoncrysol.2004.08.264.